

ffw  
H250/651

NACA TN 2343

# NATIONAL ADVISORY COMMITTEE FOR AERONAUTICS

TECHNICAL NOTE 2343

COMPARISON OF THEORETICAL AND EXPERIMENTAL RESPONSE OF  
A SINGLE-MODE ELASTIC SYSTEM IN HYDRODYNAMIC IMPACT

By Robert W. Miller and Kenneth F. Merten

Langley Aeronautical Laboratory  
Langley Field, Va.



Washington  
April 1951

Reproduced From  
Best Available Copy

20000816 136

DISTRIBUTION STATEMENT A  
Approved for Public Release  
Distribution Unlimited

AQM 00-11-3565



NATIONAL ADVISORY COMMITTEE FOR AERONAUTICS

TECHNICAL NOTE 2343

COMPARISON OF THEORETICAL AND EXPERIMENTAL RESPONSE OF  
A SINGLE-MODE ELASTIC SYSTEM IN HYDRODYNAMIC IMPACT

By Robert W. Miller and Kenneth F. Merten

SUMMARY

Hydrodynamic impact tests were made on an elastic model approximating a two-mass - spring system to determine experimentally the effects of structural flexibility on the hydrodynamic loads encountered during seaplane landing impacts and to correlate the results with theory. A flexible seaplane was represented by a two-mass - spring system consisting of a rigid prismatic float connected to a rigid upper mass by an elastic structure. The model had a ratio of sprung mass to hull mass of 0.6 and a natural frequency of 3.0 cycles per second. The tests were conducted in smooth water at fixed trims and included both high and low flight-path angles and a range of velocity.

The results of the tests are compared with theoretical time histories of hydrodynamic impact force and elastic-system response calculated by the method of NACA TN 1398 which considers the applied hydrodynamic load and structural response to be interdependent or coupled throughout the impact. The hydrodynamic-force time histories obtained with the elastic system are also compared with the hydrodynamic-force time histories that would have been obtained for the same initial conditions if the system were rigid.

These comparisons indicated that the theoretical results agreed well with the experimental results.

INTRODUCTION

Experience with large airplanes has shown that the elastic behavior of the structure during landing impact may be a critical design consideration. Analytical methods for treating landing impact of elastic structures have been developed, but most of these methods assume that the external load applied to the structure during impact is not influenced by the elasticity of the structure and that the structural response can be determined from the load that would have been applied if the structure were rigid. In reference 1, however, an analytical method for treating

hydrodynamic impact of an elastic structure is presented in which interaction of the applied load and structural response is included and it is shown that structural flexibility may have appreciable effects on the applied load.

The significant flexibility of the structure with regard to the interaction between structural response and hydrodynamic force is considered in reference 1 to be the flexure of the fuselage-wing structure in the fundamental mode. This structural action was shown to be represented by a two-mass - spring system having the same frequency as the fundamental mode of the represented structure and a mass ratio determined by the physical characteristics of the structure being represented.

Since no adequate experimental check of the method presented in reference 1 had been made, water impact tests of an elastic model approximating a two-mass - spring system were made at the Langley impact basin. The results of these tests and a comparison with theory are presented in this paper in the form of acceleration time histories for the center of gravity and for the structural response.

#### SYMBOLS

|            |  |
|------------|--|
| $g$        | acceleration due to gravity  |
| $m_j$      | mass at spanwise station $j$   |
| $m_L$      | lower, or hull, mass of two-mass system  |
| $m_S$      | upper, or sprung, mass of two-mass system  |
| $n_i$      | impact acceleration of center of gravity normal to water surface, $g$                          |
| $n_S$      | sprung, or upper, mass acceleration normal to water surface, $g$                               |
| $t_i$      | time between initial contact and maximum hydrodynamic force for the structure considered rigid |
| $t_n$      | time required for one-fourth cycle of natural vibration  |
| $V_o$      | resultant velocity at instant of contact with water surface                                    |
| $\gamma_o$ | flight-path angle at contact   |
| $\tau$     | angle of trim, angle of keel relative to water surface   |

$\phi_j$  ratio of deflection of fundamental mode at station  $j$  to deflection at center line

## APPARATUS

Basin.- A sketch giving the general arrangement of the Langley impact basin and equipment is presented in figure 1. Briefly, the operation of the equipment is as follows: The carriage, to which the model is attached by means of a parallelogram drop linkage, is catapulted at the desired horizontal velocity and then allowed to coast along the tank rails to the test section. At the test section the drop linkage is released and the model, under the action of gravity, attains the required vertical velocity, at which time the lift engine applies to it an upward force which simulates any desired constant wing lift throughout the impact. A more detailed description of this standard Langley impact basin equipment is given in reference 2.

Model.- Views of the model used in the tests are presented in figure 2. A flexible beam (referred to as the elastic wing or the wing) was rigidly attached at its midspan to the vertical member or boom of the drop linkage. This wing was symmetrical in construction about the midspan and had a group of lead weights attached near each tip equidistant from the midspan. Directly beneath the wing midspan a dynamometer truss and float model were rigidly attached in such a way that the float keel and the wing chord remained parallel for all model trims.

In order to prevent unwanted oscillations during catapulting and dropping of the model, the tips of the wing were rigidly linked to the float during these phases by means of loose-fitting telescoping tubes (figs. 2(a), 2(b), and 3(a)) which were pinned to prevent motion. The pins were released by a cable system immediately before water contact, at which time the model was in a state of constant velocity translation with no forces being transmitted by the telescoping tubes.

The hydrodynamic considerations of reference 1 assume immersion of a V-bottom float without chine immersion. To prevent chine immersion with the dropping weight (2400 lb) used in the present tests, it was necessary to extend the bottom of the float (figs. 2(b) and 3(a)). Otherwise the float used was the same as the forebody of the float described in reference 3.

Instrumentation.- The standard carriage instrumentation, described in reference 2, was used to measure time histories of the lift force and of the horizontal and vertical components of velocity and displacement.

Time histories of vertical acceleration were measured by strain-gage accelerometers located on the boom and on the wing near the tips at about the center of gravity of each half of the tip weights. Since the tip accelerometers were mounted vertically on the wing at zero model trim, the direction of the tip-mass accelerations actually differed from the vertical as influenced by the model trim angle, but the difference is negligible.

As previously mentioned, a dynamometer truss was mounted between the float and the wing (fig. 3(a)). The load-measuring part of the truss was a tubular structure with vertical, horizontal, and transverse members oriented so that they were subject to the respective force reactions at the support points. Wire strain gages were mounted on the tubes and each installation was enclosed within a hermetically sealed metal bellows.

Control-position transmitters were mounted on the telescoping tubes in such a way that the relative displacement of the wing tips to the float could be measured. The records obtained from these transmitters were used to aid in checking the frequency and symmetry of the wing-tip oscillations.

#### EQUIVALENT TWO-MASS - SPRING SYSTEM

The elastic model (fig. 3(a)) used in the present tests was constructed to approximate as closely as possible a two-mass - spring system as defined in reference 1. The elastic wing served as the spring of the system and, to prevent as nearly as possible the occurrence of higher modes, the wing was constructed to weigh as little as possible. The hull, boom, and dynamometer truss made up most of the lower or hull mass; the lead weights near the wing tips made up most of the two halves of the upper or sprung mass.

The amount of the wing weight apportioned to each mass and the resulting mass ratio of the system were determined by the following calculations. With the use of the actual mass distribution of the model (with the weight of the telescoping tubes divided between the hull and wing tip) and the known stiffness distribution of the wing, the fundamental free-free mode of the system was calculated by the method of reference 4. With this mode and mass distribution, see figure 3(b), the mass ratio of the equivalent two-mass - spring system was computed by means of the following equation, which is another form of equation (B6) of reference 1:

$$\frac{m_S}{m_L} = \frac{\sum m_j}{\sum m_j \phi_j^2}$$

where  $m_j$  is the mass at a spanwise station  $j$  and  $\phi_j$  is the ratio of the deflection of the fundamental mode at station  $j$  to the deflection at the center line. The mass ratio was determined to be 0.6 and, since the total weight was 2400 pounds, the equivalent lower and upper masses weighed 1500 and 900 pounds, respectively; thus, the equivalent system is that shown in figure 3(c).

As a check on the nodal-point position and frequency of the mode of the elastic model which was used to calculate the equivalent mass ratio, a series of drops of the elastic model was made with the carriage standing still to obtain the natural frequency and nodal-point positions of the elastic model. The lift engine was set to balance the weight of the model during most of the drop and thereby simulate the conditions existing during the test runs. In this manner about 3 cycles of oscillation were obtained before the model contacted the water. The records of both the control-position transmitters and the wing-tip accelerometers showed that the computed value for natural frequency was correct. An accelerometer which was moved between drops along one-half the wing span in increments of 2 inches from one side of the computed nodal point to the other showed a definite reversal in phase of the oscillations and the nodal point was thereby determined to be, within the margin of error involved, in agreement with the computed value.

In the two-mass - spring system used in reference 1 to represent the fundamental mode of vibration of an airplane, the vibratory motion is considered to be in a direction perpendicular to the keel of the float. The elastic wing used in the present tests restrained the tip mass so that it vibrated in a direction perpendicular to the plane of the elastic wing and hence perpendicular to the keel; therefore, the conditions of the theoretical system of reference 1 are satisfied. However, the parallelogram drop linkage restricted the lower-mass motion to the vertical direction. This condition introduced an effective increase in mass in the direction perpendicular to the keel for trim angles not equal to zero, but the increase was found to be negligible for the present tests as the angles involved are small.

#### TEST PROCEDURE AND PRECISION OF DATA

In accordance with the assumptions made for the theoretical solutions in reference 1, the tests were made in smooth water with the lift engine set to simulate wing lift equal to the dropping weight (2400 lb).

Part of the tests were made at a trim of  $3^\circ$  and a flight-path angle of approximately  $14^\circ$ , and the rest of the tests were made at  $9^\circ$  trim and approximately  $6^\circ$  flight-path angle. The tests for each combination of trim and flight-path angle were set up to give as wide a range of the

dimensionless ratio  $t_n/t_i$  as the test equipment would allow. Since the natural period of the model is fixed and since the flight-path angle was held constant during each group of tests, the variation of  $t_n/t_i$  was obtained by varying the resultant velocity of the model at water contact and thereby varying the impact-load duration. The resultant velocities used and  $t_n/t_i$  values obtained are shown in table I.

The apparatus and instrumentation used in the tests give measurements which are believed to be accurate within the following limits:

|  |        |
|--|--------|
| Horizontal velocity, feet per second . . . . . | ±0.5   |
| Vertical velocity, feet per second . . . . .   | ±0.2   |
| Weight, pounds . . . . .                       | ±2.0   |
| Acceleration, g . . . . .                      | ±0.2   |
| Time, seconds . . . . .                        | ±0.005 |
| Vertical force, pounds . . . . .               | ±200.0 |

The plots of figure 4 are included as an indication of the consistency of the experimental data. Each of the two plots represents a group of runs having initial conditions the same within instrument error and shows for each run the center-of-gravity acceleration and the wing-tip or sprung-mass acceleration. The center-of-gravity acceleration was obtained as follows: The product of the recorded lower-mass acceleration and the float mass was added to the recorded truss-force time history to obtain the true hydrodynamic force. This value was then divided by the total mass of the system to obtain the center-of-gravity acceleration.

It may be seen from the plots that the center-of-gravity acceleration peaks have a random scatter of about 0.1g (5 percent) and the sprung-mass acceleration peaks have a corresponding scatter of less than 0.2g (7 percent).

The peaks of the left and right halves of the sprung mass for any one run also disagree by about 7 percent. The plots of figures 4 and 5, and also other runs, indicate, however, that there is no consistent disagreement among runs; for some runs the peak of the left half is lower than the right half and vice versa. This disagreement for any one run and this inconsistency between runs of the sprung-mass peaks have not been definitely accounted for but may be due to use of the telescoping tubes.

## RESULTS AND DISCUSSION

In order to summarize the results, a tabulation is presented in table I of the test conditions, peak theoretical and experimental



accelerations, and the period ratio  $t_n/t_i$  for all the runs. The test conditions are defined by the flight-path angle and resultant velocity at water contact,  $\gamma_0$  and  $V_0$ , respectively, and by the model trim angle  $\tau$ . The theoretical and experimental results presented in this table are the maximum values of the center-of-gravity and sprung-mass accelerations of the two-mass - spring system together with theoretical center-of-gravity accelerations for a rigid system of the same total mass at the same initial conditions. Because of the lengthy calculations required for the theoretical solution of the elastic system, theoretical results were found for only six runs.

For these six runs, figure 5 presents time-history comparisons of the experimental and theoretical accelerations for the center of gravity and for the response of a two-mass - spring system during impact. The theoretical hydrodynamic-force time histories that would have been obtained for the same initial conditions if the system were rigid are also presented. These comparisons exemplify most of the range of  $t_n/t_i$  tested for both the high- and low-flight-path regions. The theoretical solutions for the elastic body were computed by the method of reference 1, except that the parameter describing the virtual mass (parameter A in appendix A of reference 1) was modified by changing the constant 0.82 (contained in the parameter) to 1.00 in accord with Wagner, reference 5, and the later theoretical and experimental developments presented in reference 6. This constant, which is at present still controversial for the dead-rise angle considered herein, changes the results by about 3 percent and hence for the purpose of the present paper is not of great importance. The rigid-body curves were obtained by use of the method of reference 3.

The plots of figure 5 show that the experimental time history of center-of-gravity acceleration for the elastic system is quite well represented by the corresponding theoretical time history. The experimental curves in general have a slight time lag with respect to the computed curves and the maximum values of acceleration are within  $\pm 6$  percent of the maximum computed accelerations, which is within the range of experimental scatter as shown in figure 4.

By comparing these curves with the curves for the rigid-body center-of-gravity acceleration, it may be seen that the reduction in maximum acceleration due to the elasticity of the structure is of the order of 20 percent. More cases may be considered by comparing the experimental results with the theoretical rigid-body results in table I and it may be seen that this reduction may vary from 6 to 25 percent. These results, of course, represent only particular values of the period ratio  $t_n/t_i$  and the mass ratio  $m_S/m_L$ . For other ranges of these ratios the peak center-of-gravity acceleration may be further reduced or it may even be increased up to 10 or 12 percent above the rigid-body acceleration

(reference 1). The values of the period ratio  $t_n/t_1$  and the mass ratio  $m_S/m_L$  used in the present tests were selected to give the relatively large reductions (up to 25 percent) in center-of-gravity accelerations that were obtained. The large differences in elastic and rigid-body center-of-gravity accelerations compared with the small differences between the theoretical and experimental elastic-body center-of-gravity accelerations make the agreement of the theoretical values with experimental values more significant than if the elastic- and rigid-body results were more nearly equal.

From the comparison of the experimental and theoretical time-history curves for sprung-mass accelerations it appears that the maximum theoretical accelerations are larger than the experimental accelerations throughout the impact for all conditions tested. This difference may be due to damping, which is not taken into account in the theoretical analysis. Damping was observed in the drop tests made to verify the computed natural frequency and a rough analysis of the effects of this damping indicated that the discrepancy between the computed and experimental results could be approximately attributed to it.

#### CONCLUSIONS

Hydrodynamic impact tests were made on an elastic model approximating a two-mass - spring system which had a ratio of sprung mass to hull mass of 0.6 and a natural frequency of 3.0 cycles per second. One group of tests was made at a trim of  $3^\circ$  and a flight-path angle of approximately  $14^\circ$  and another group of tests was made at a trim of  $9^\circ$  and a flight-path angle of approximately  $6^\circ$ . A period ratio (the ratio of one-quarter the natural period of the elastic model to the time between initial contact and maximum hydrodynamic force for the structure considered rigid) ranging from 0.43 to 1.54 was covered. Comparison of the results with theory indicated the following conclusions:

1. Theoretical time histories of the center-of-gravity acceleration obtained by the method of NACA TN 1398 agree with the experimental results within the range of scatter of the data.

2. Theoretical time histories of acceleration associated with elastic structural response obtained by the method of NACA TN 1398 agree with the experimental results within a range of error which may be attributed to damping.

Langley Aeronautical Laboratory  
National Advisory Committee for Aeronautics  
Langley Field, Va., January 30, 1951

## REFERENCES

1. Mayo, Wilbur L.: Solutions for Hydrodynamic Impact Force and Response of a Two-Mass System with an Application to an Elastic Airframe. NACA TN 1398, 1947.
2. Batterson, Sidney A.: The NACA Impact Basin and Water Landing Tests of a Float Model at Various Velocities and Weights. NACA Rep. 795, 1944.
3. Mayo, Wilbur L.: Theoretical and Experimental Dynamic Loads for a Prismatic Float Having an Angle of Dead Rise of  $22\frac{1}{2}^{\circ}$ . NACA RB L5F15, 1945.
4. Houbolt, John C., and Anderson, Roger A.: Calculation of Uncoupled Modes and Frequencies in Bending or Torsion of Nonuniform Beams. NACA TN 1522, 1948.
5. Wagner, Herbert: Über Stoss- und Gleitvorgänge an der Oberfläche von Flüssigkeiten. Z.f.a.M.M., Bd. 12, Heft 4, Aug. 1932, pp. 193-215.
6. Milwitzky, Benjamin: A Generalized Theoretical and Experimental Investigation of the Motions and Hydrodynamic Loads Experienced by V-Bottom Seaplanes during Step-Landing Impacts. NACA TN 1516, 1948.

TABLE I  
TEST DATA AND THEORETICAL PEAK VALUES FOR HYDRODYNAMIC  
IMPACT OF A TWO-MASS - SPRING SYSTEM

| Run              | Initial conditions |                     | Period ratio      | Rigid body  |                      | Elastic body         |                      |                      |  |
|------------------|--------------------|---------------------|-------------------|-------------|----------------------|----------------------|----------------------|----------------------|--|
|                  | $V_0$<br>(fps)     | $\gamma_0$<br>(deg) |                   | Theoretical | $n_{i_{max}}$<br>(g) | Theoretical<br>(a)   |                      | Experimental         |  |
|                  |                    |                     | $\frac{t_n}{t_1}$ |             | $n_{i_{max}}$<br>(g) | $n_{s_{max}}$<br>(g) | $n_{i_{max}}$<br>(g) | $n_{s_{max}}$<br>(g) |  |
| $\tau = 3^\circ$ |                    |                     |                   |             |                      |                      |                      |                      |  |
| 1                | 23.4               | 12.31               | 0.76              | 0.8         | ---                  | ---                  | 0.6                  | 1.0                  |  |
| 2                | 23.9               | 13.55               | .83               | 1.0         | ---                  | ---                  | .7                   | 1.1                  |  |
| 3                | 24.2               | 11.91               | .78               | .8          | ---                  | ---                  | .6                   | .9                   |  |
| 4                | 26.7               | 13.51               | .94               | 1.2         | 1.0                  | 1.7                  | .9                   | 1.5                  |  |
| 5                | 27.3               | 13.51               | .96               | 1.3         | ---                  | ---                  | .7                   | 1.6                  |  |
| 6                | 32.9               | 14.43               | 1.34              | 2.1         | 1.6                  | 2.6                  | 1.6                  | 2.1                  |  |
| 7                | 33.5               | 14.28               | 1.24              | 2.1         | ---                  | ---                  | 1.6                  | 2.3                  |  |
| 8                | 33.7               | 14.33               | 1.26              | 2.1         | ---                  | ---                  | 1.6                  | 2.3                  |  |
| 9                | 38.2               | 8.79                | .90               | 1.2         | ---                  | ---                  | .9                   | 1.6                  |  |
| 10               | 38.9               | 14.09               | 1.44              | 2.9         | 2.1                  | 3.1                  | 2.0                  | 2.6                  |  |
| 11               | 39.2               | 13.97               | 1.44              | 2.8         | ---                  | ---                  | 2.0                  | 2.6                  |  |
| 12               | 42.5               | 13.84               | 1.54              | 3.2         | ---                  | ---                  | 2.5                  | 3.0                  |  |
| $\tau = 9^\circ$ |                    |                     |                   |             |                      |                      |                      |                      |  |
| 13               | 32.5               | 5.79                | 0.43              | 0.6         | ---                  | ---                  | 0.5                  | 0.5                  |  |
| 14               | 38.3               | 4.81                | .45               | .6          | ---                  | ---                  | .5                   | .8                   |  |
| 15               | 48.5               | 6.41                | .69               | 1.4         | ---                  | ---                  | 1.3                  | 2.1                  |  |
| 16               | 49.7               | 5.85                | .67               | 1.3         | 1.1                  | 2.0                  | 1.2                  | 1.7                  |  |
| 17               | 58.8               | 5.52                | .75               | 1.7         | ---                  | ---                  | 1.4                  | 2.1                  |  |
| 18               | 58.8               | 5.87                | .79               | 1.9         | 1.5                  | 2.5                  | 1.6                  | 2.3                  |  |
| 19               | 67.0               | 5.66                | .89               | 2.4         | 1.8                  | 3.0                  | 1.9                  | 2.6                  |  |
| 20               | 67.2               | 5.69                | .89               | 2.3         | ---                  | ---                  | 1.8                  | 2.6                  |  |
| 21               | 67.9               | 5.48                | .87               | 2.3         | ---                  | ---                  | 1.9                  | 2.8                  |  |
| 22               | 80.8               | 3.76                | .82               | 2.0         | ---                  | ---                  | 1.6                  | 2.2                  |  |

<sup>a</sup>Values obtained only for runs used in figure 5.



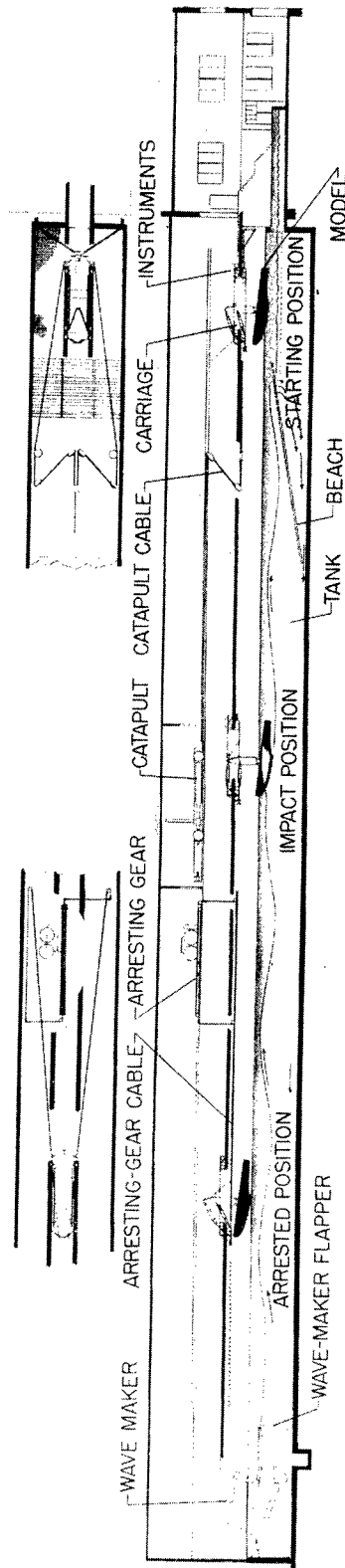
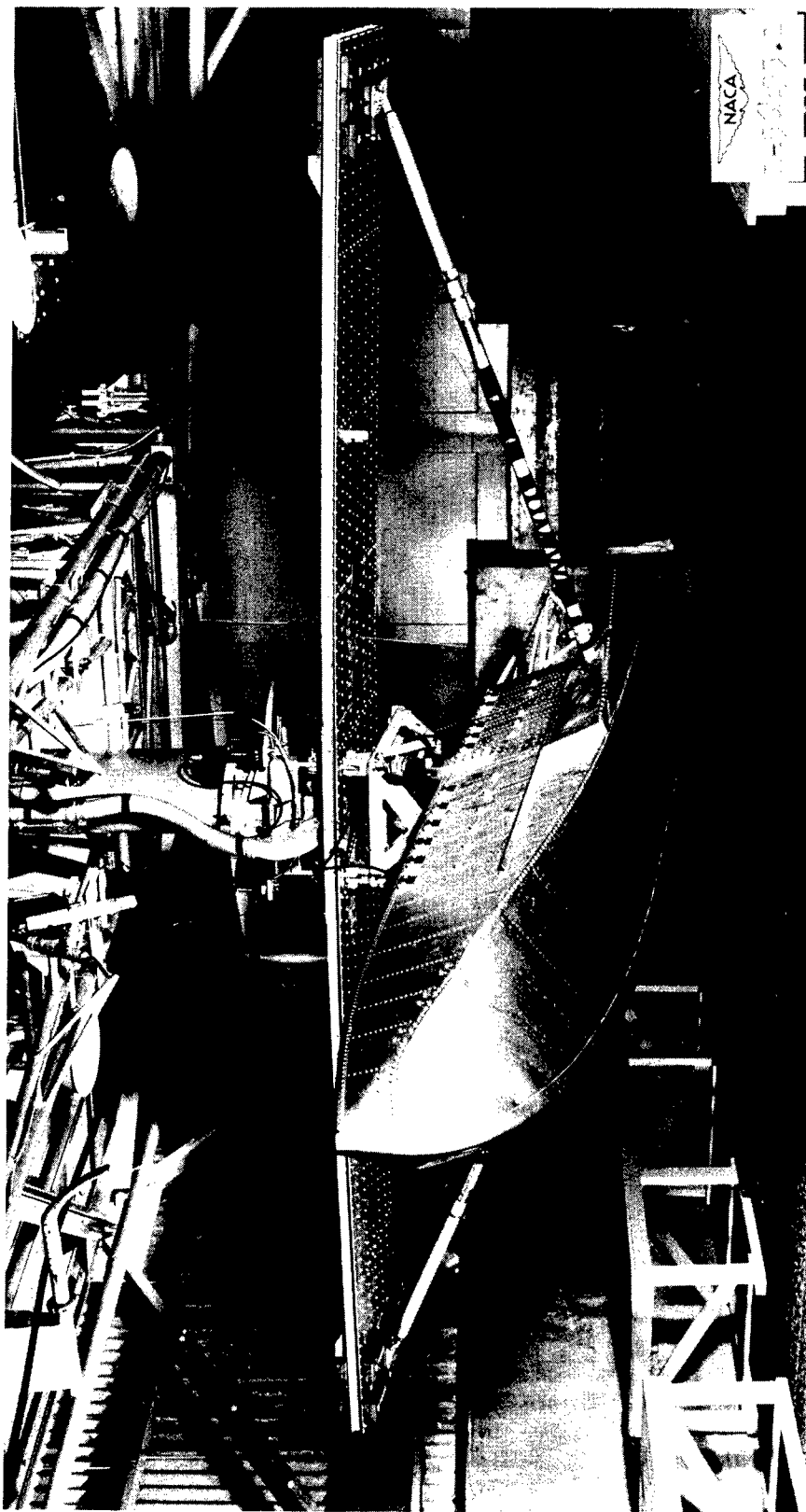


Figure 1.- Sketch of Langley impact basin. Length, 360 feet; width, 24 feet; depth, 11 feet; water depth, 8 feet.

NACA  
L-49297.1



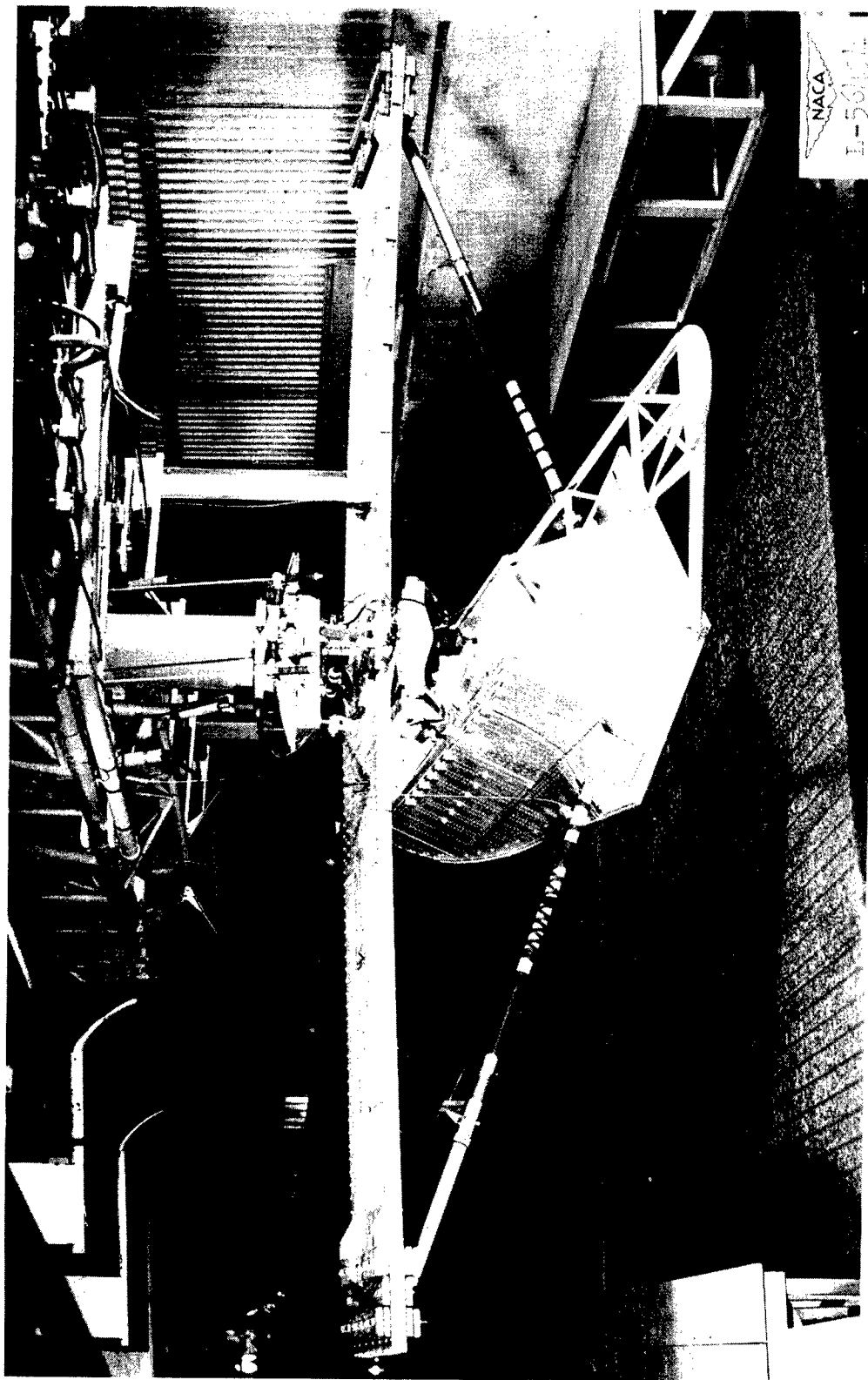


(a) Front one-quarter view.

Figure 2.- Photographs of the model.

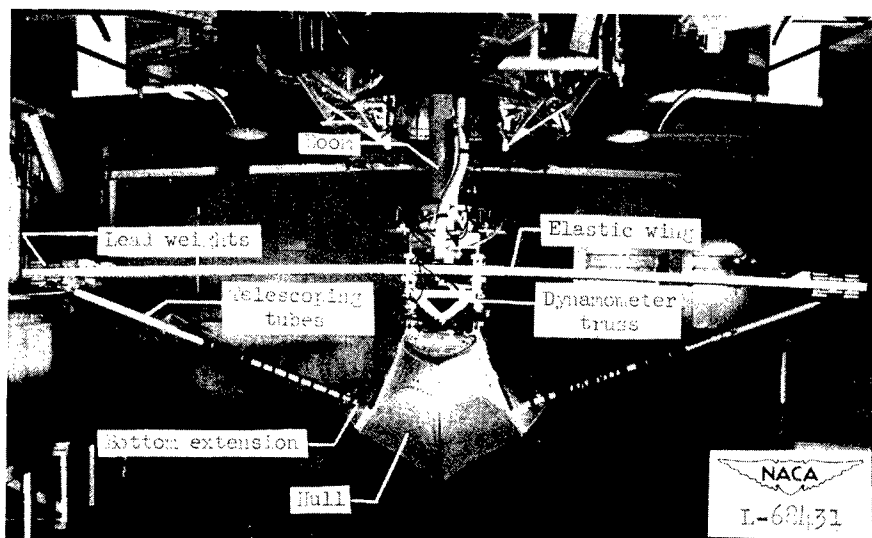




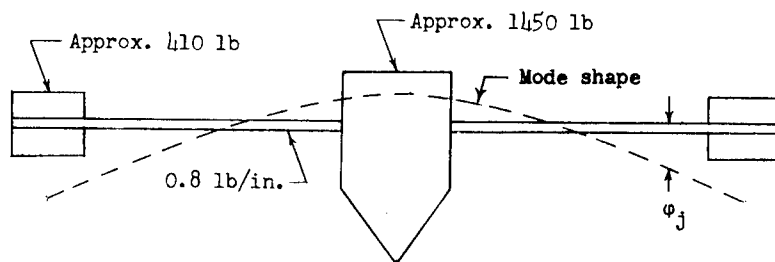


(b) Rear one-quarter view.

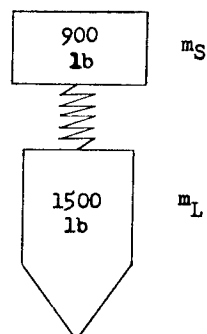
Figure 2.- Concluded.



(a) Test system. Wing span 216 inches.

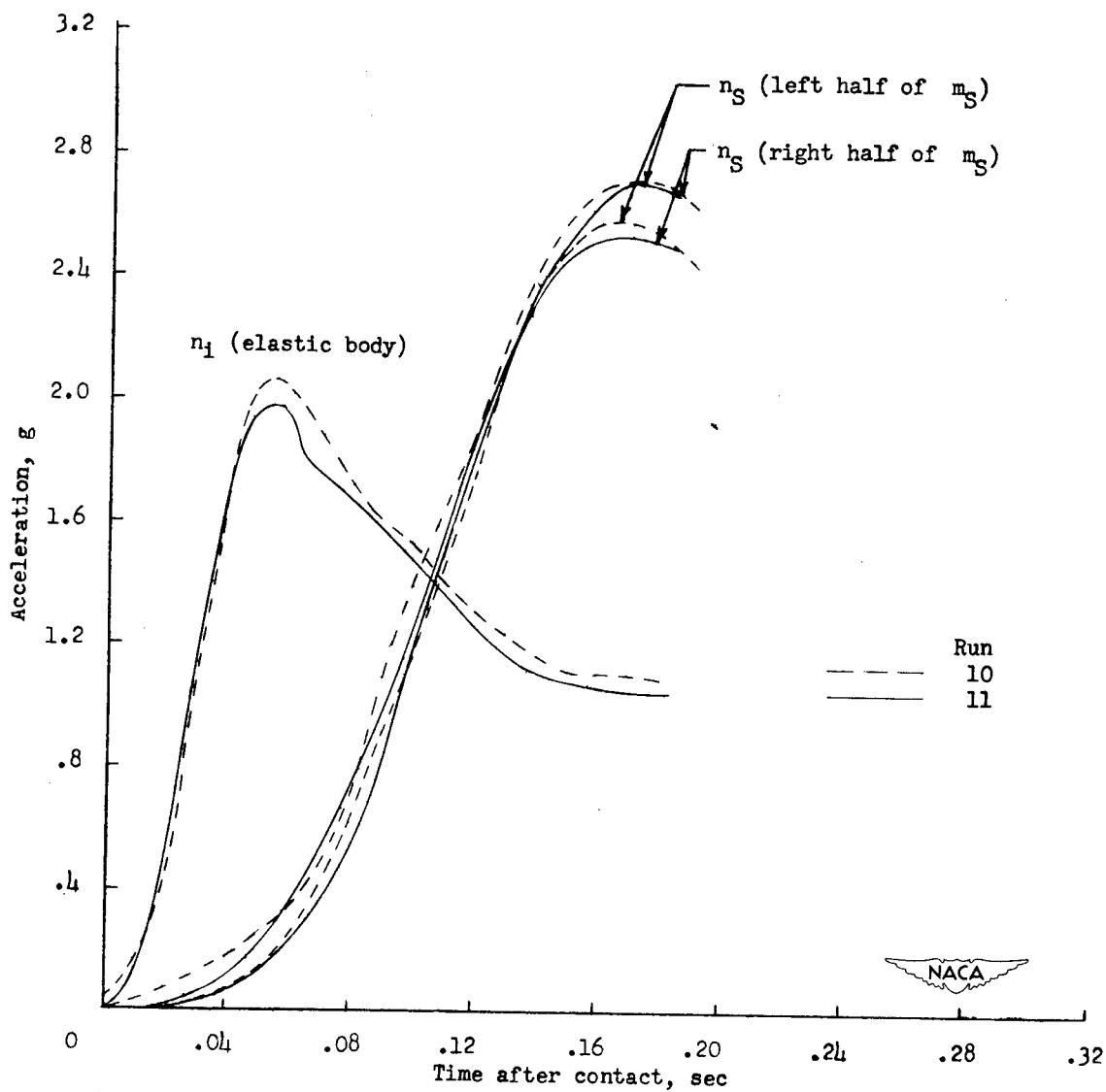


(b) Effective test system.



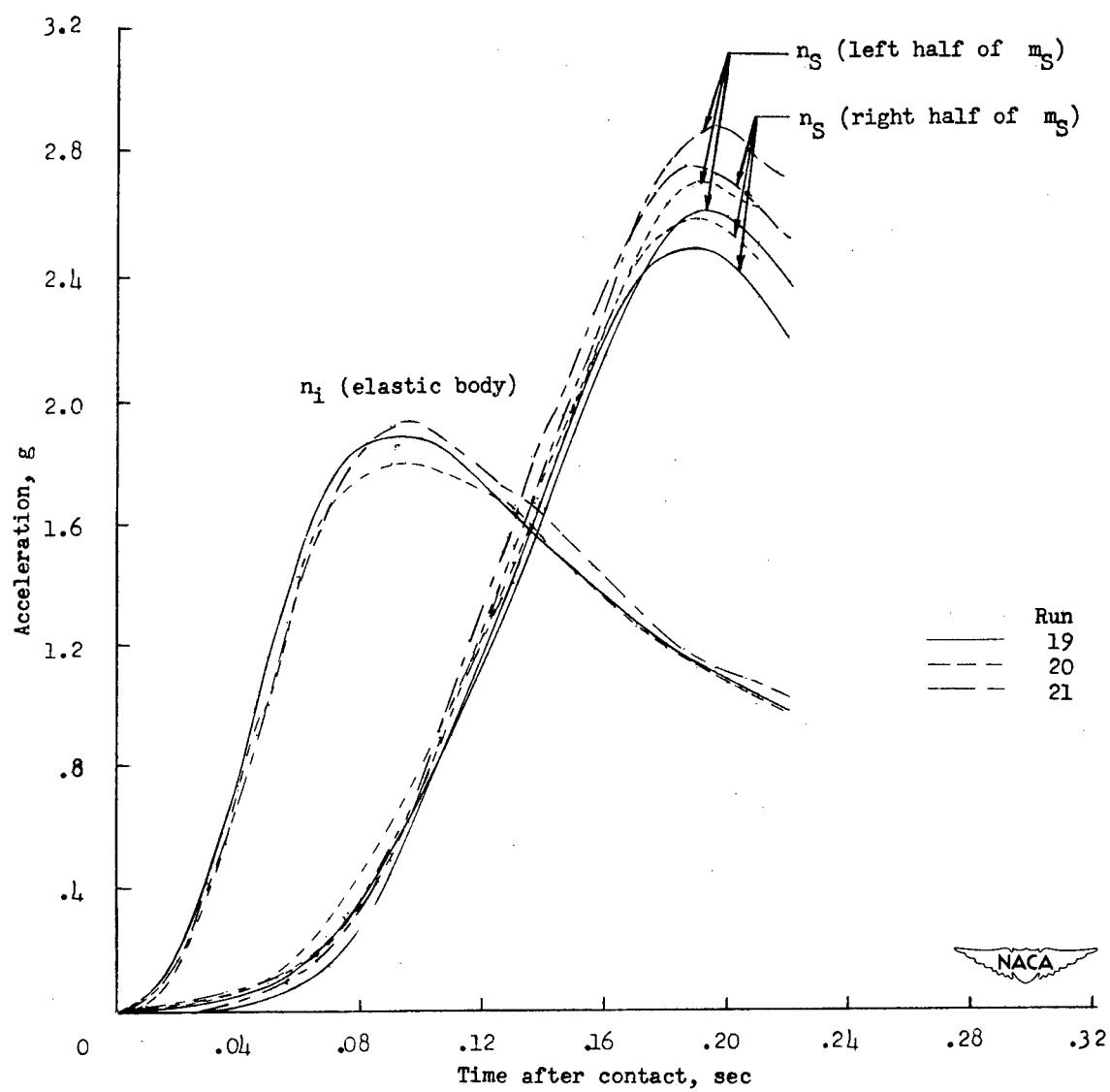
(c) Equivalent two-mass - spring system.  $\frac{m_S}{m_L} = 0.6$ ; natural frequency, 3 cycles per second.

Figure 3.- Equivalence of experimental and theoretical systems.



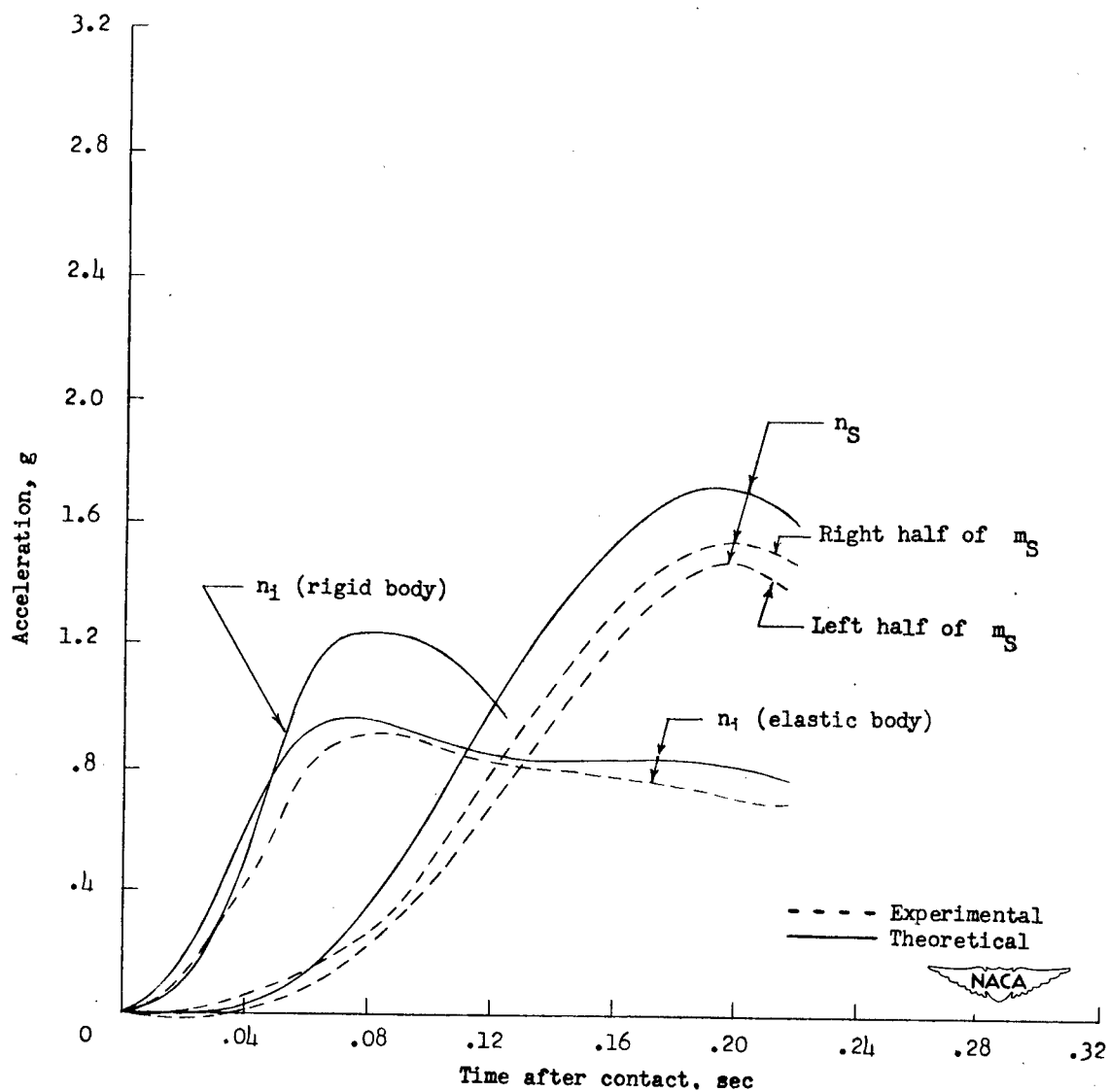
(a)  $\tau = 3^\circ$ ;  $\gamma_0 \approx 14^\circ$ .

Figure 4.- Consistency of experimental data.



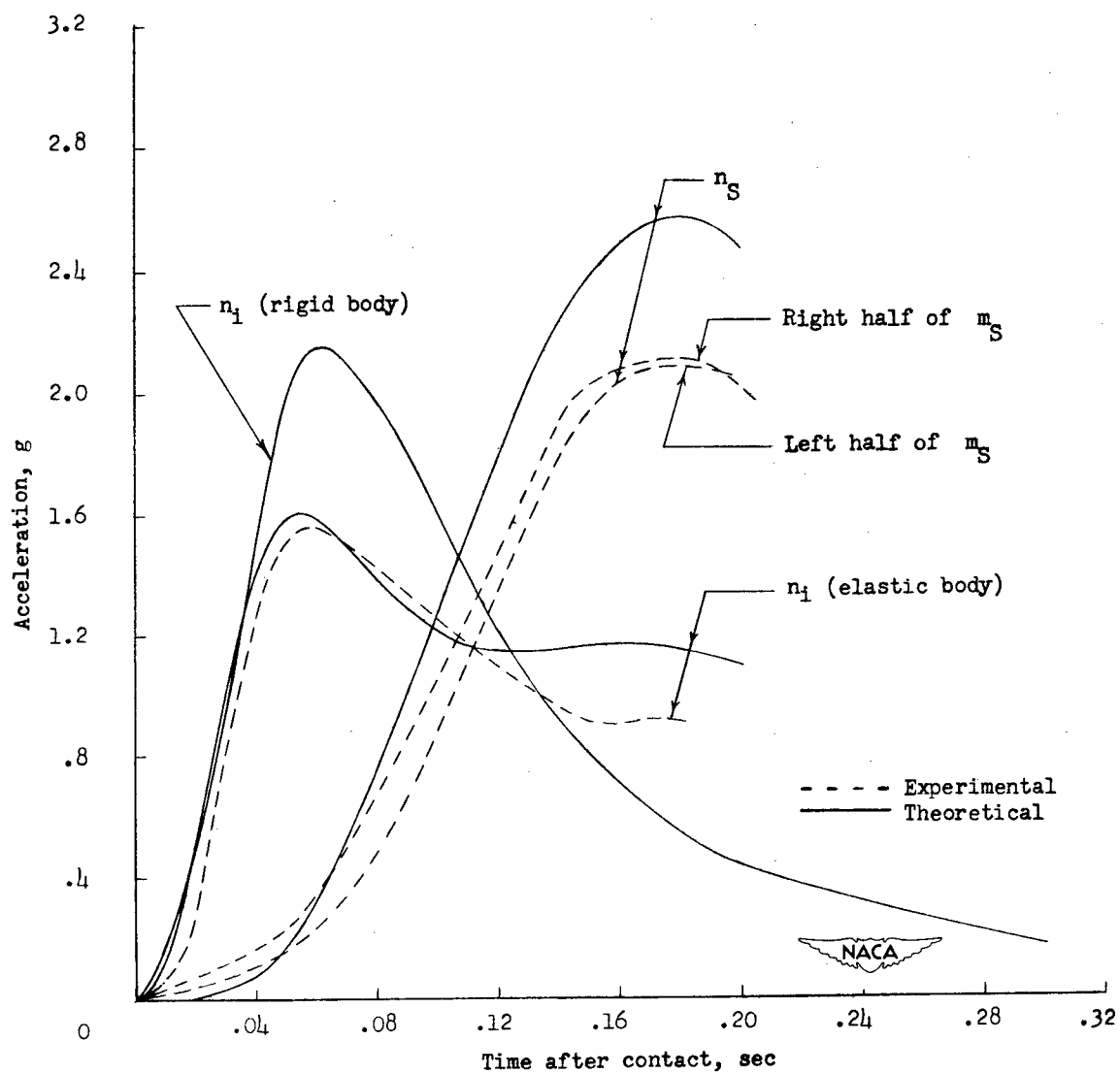
(b)  $\tau = 9^\circ$ ;  $\gamma_0 \approx 6^\circ$ .

Figure 4.- Concluded.



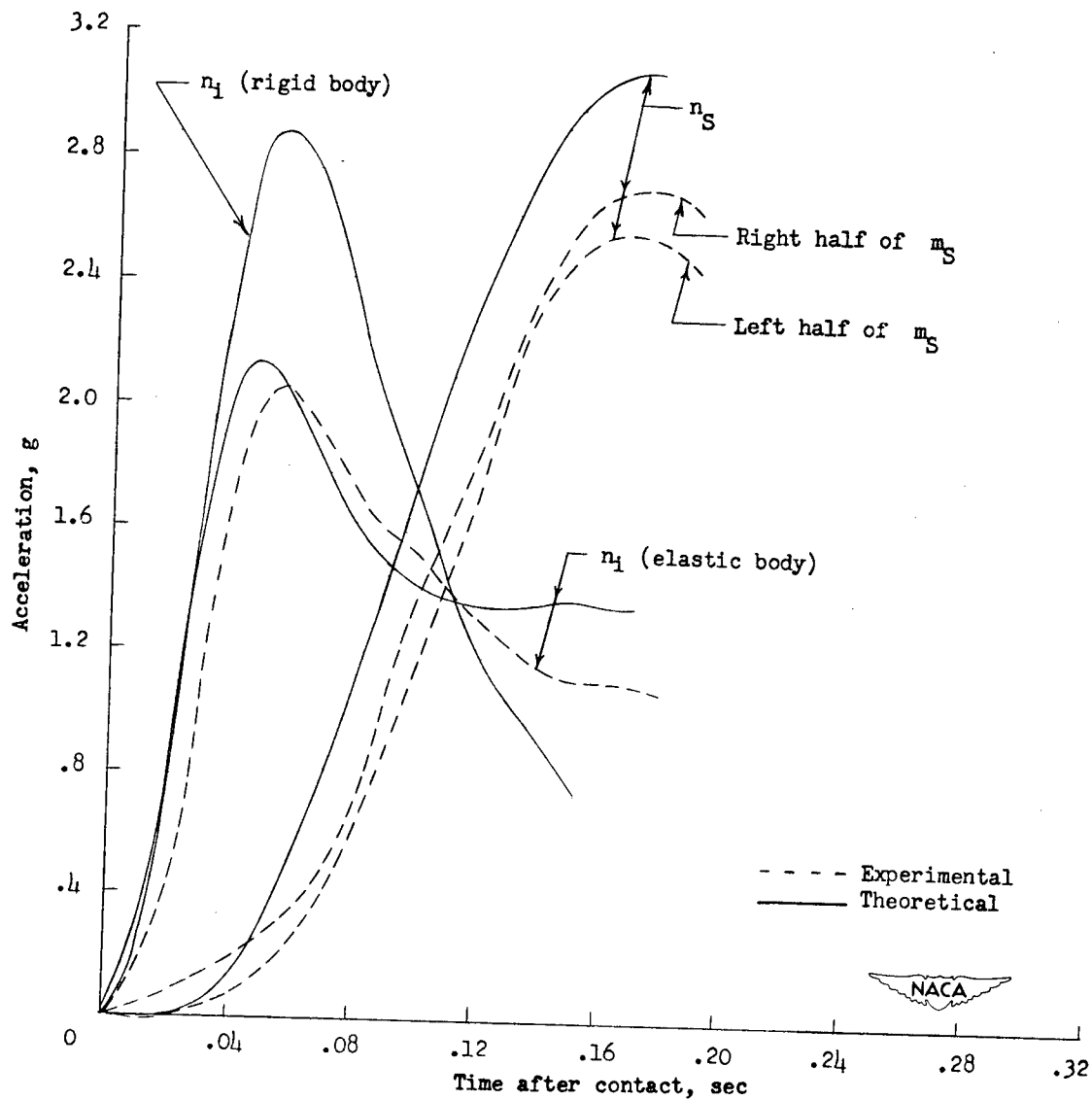
(a) Run 4:  $\tau = 3^\circ$ ,  $\gamma_0 = 13.51^\circ$ ,  $\frac{t_n}{t_i} = 0.94$ ,  $V_0 = 26.7$  feet per second.

Figure 5.- Comparison of theoretical and experimental hydrodynamic impact force and response of a two-mass - spring system.



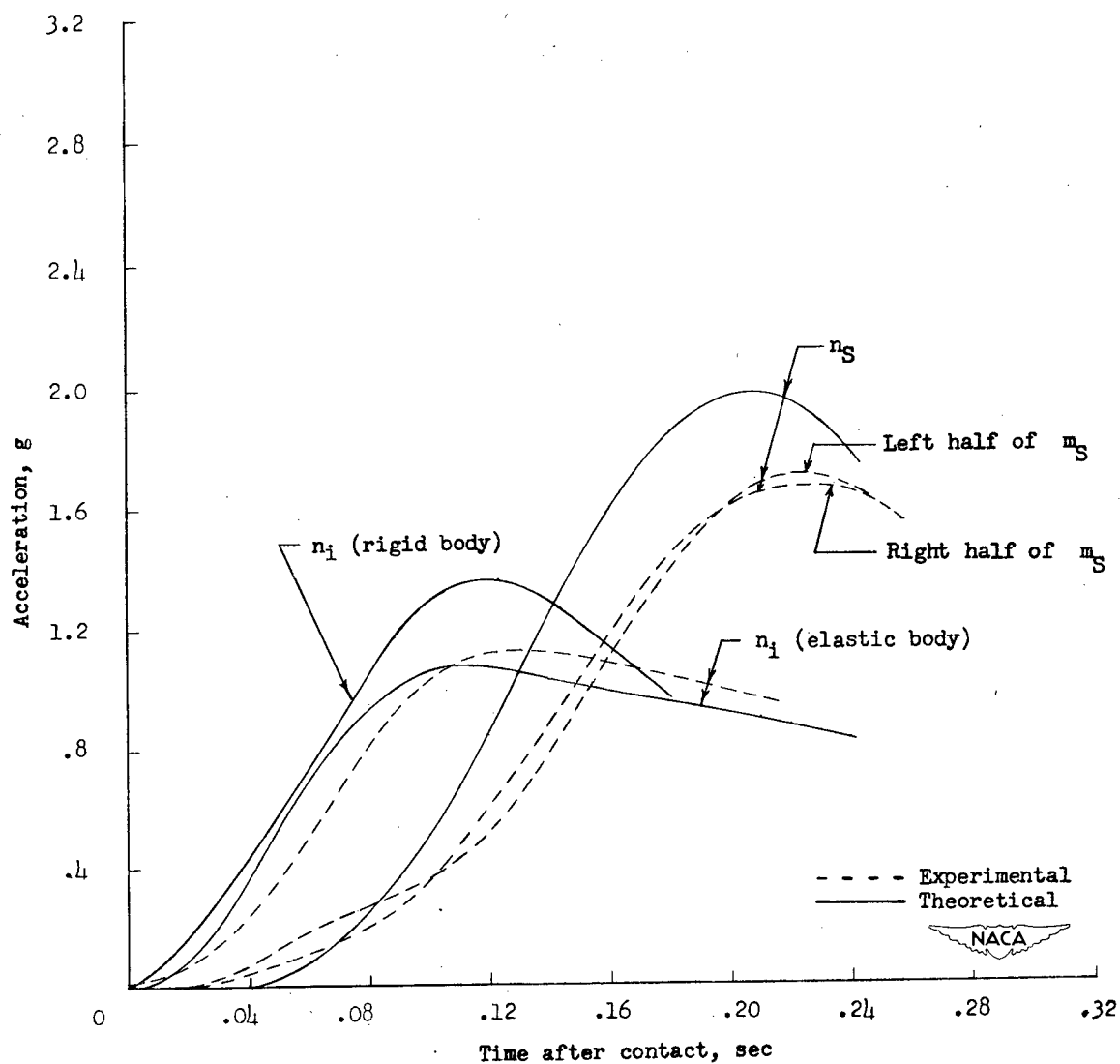
(b) Run 6:  $\tau = 3^\circ$ ,  $\gamma_0 = 14.43^\circ$ ,  $\frac{t_n}{t_i} = 1.34$ ,  $V_0 = 32.9$  feet per second.

Figure 5.- Continued.



(c) Run 10:  $\tau = 3^\circ$ ,  $\gamma_0 = 14.09^\circ$ ,  $\frac{t_n}{t_i} = 1.44$ ,  $V_0 = 38.9$  feet per second.

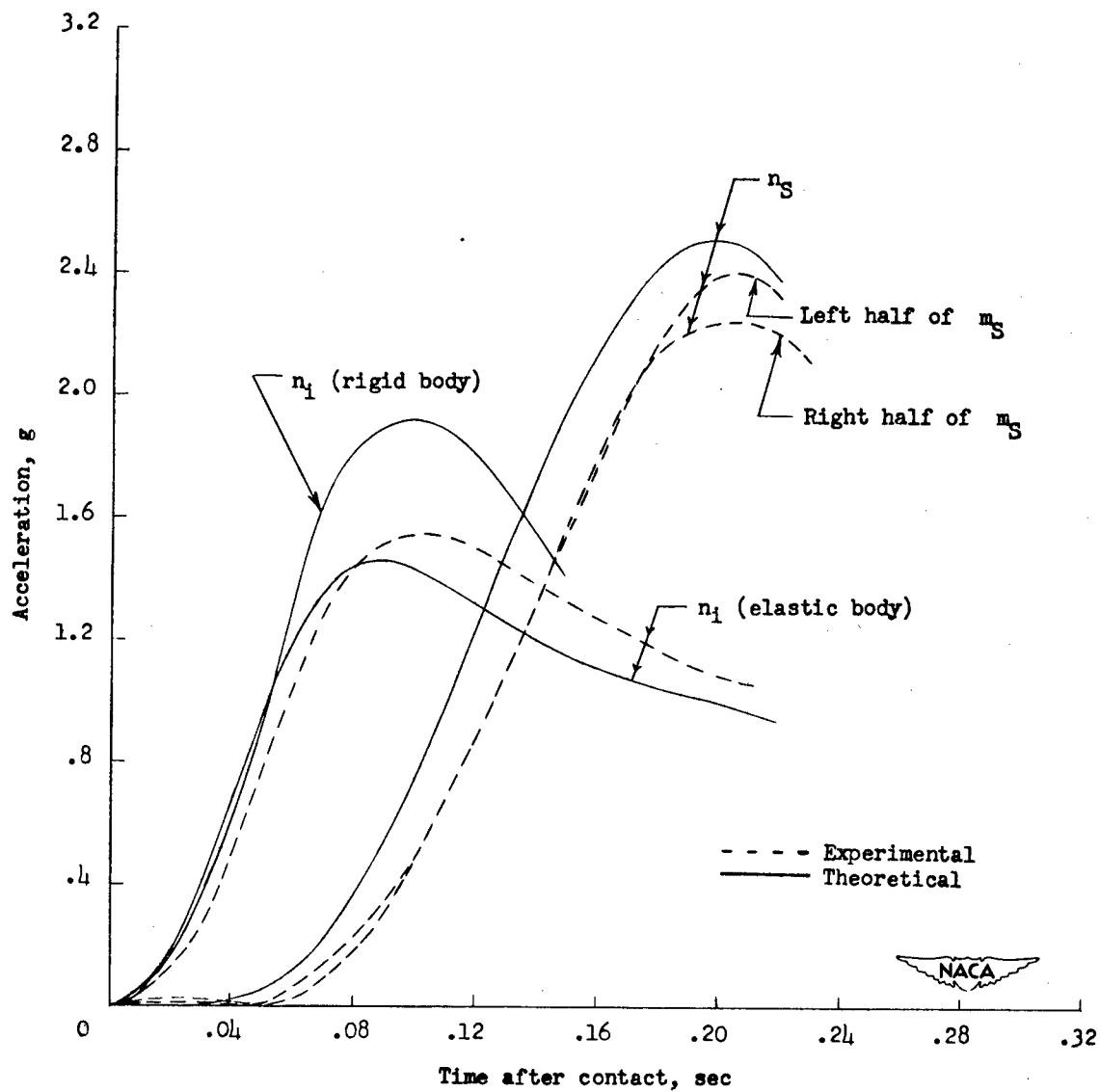
Figure 5.- Continued.



(d) Run 16:  $\tau = 9^\circ$ ,  $\gamma_0 = 5.85^\circ$ ,  $\frac{t_n}{t_i} = 0.67$ ,  $V_0 = 49.7$  feet per second

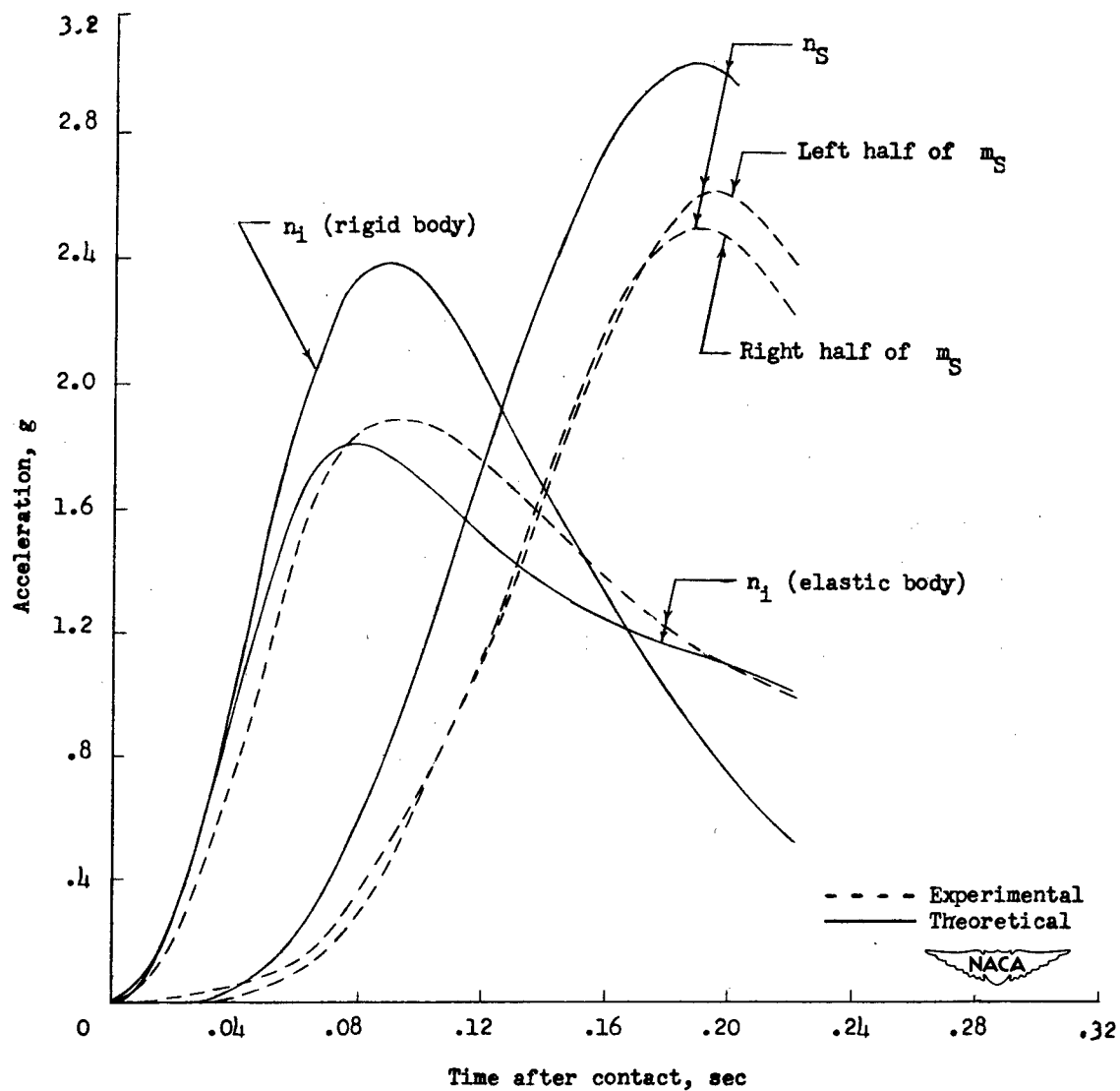
Figure 5.- Continued.





(e) Run 18:  $\tau = 9^\circ$ ,  $\gamma_0 = 5.87^\circ$ ,  $\frac{t_n}{t_i} = 0.79$ ,  $V_0 = 58.8$  feet per second.

Figure 5.- Continued.



(f) Run 19:  $\tau = 9^\circ$ ,  $\gamma_0 = 5.66^\circ$ ,  $\frac{t_n}{t_i} = 0.89$ ,  $V_0 = 67.0$  feet per second.




Figure 5.- Concluded.

Abstract

Hydrodynamic impact tests were made on an elastic model approximating a two-mass - spring system which had a ratio of sprung mass to hull mass of 0.6 and a natural frequency of 3.0 cycles per second. Tests were made at two combinations of trim and flight-path angles and for a range of flight-path velocity. Comparison of the experimental results with results obtained from the theory of NACA TN 1398 showed good agreement.

Abstract

Hydrodynamic impact tests were made on an elastic model approximating a two-mass - spring system which had a ratio of sprung mass to hull mass of 0.6 and a natural frequency of 3.0 cycles per second. Tests were made at two combinations of trim and flight-path angles and for a range of flight-path velocity. Comparison of the experimental results with results obtained from the theory of NACA TN 1398 showed good agreement.

|   |  |
|---|--|
| <p>Hydrodynamics</p> <hr/> <p style="text-align: center;"> NACA</p> <hr/> <p>Comparison of Theoretical and Experimental Response of a Single-Mode Elastic System in Hydrodynamic Impact.</p> <p>By Robert W. Miller and Kenneth F. Merten</p> <p>NACA TN 2343<br/>April 1951</p> <p style="text-align: right;">(Abstract on Reverse Side)</p>                    | <p>2</p> <hr/> <p style="text-align: center;"> NACA</p> <hr/> <p>Comparison of Theoretical and Experimental Response of a Single-Mode Elastic System in Hydrodynamic Impact.</p> <p>By Robert W. Miller and Kenneth F. Merten</p> <p>NACA TN 2343<br/>April 1951</p> <p style="text-align: right;">(Abstract on Reverse Side)</p> |
| <p>Loads, Landing -<br/>Impact, Water</p> <hr/> <p style="text-align: center;"> NACA</p> <hr/> <p>Comparison of Theoretical and Experimental Response of a Single-Mode Elastic System in Hydrodynamic Impact.</p> <p>By Robert W. Miller and Kenneth F. Merten</p> <p>NACA TN 2343<br/>April 1951</p> <p style="text-align: right;">(Abstract on Reverse Side)</p> | <p>4.1.2.1.2</p>   |